JARO 13: 323–333 (2012)
DOI: 10.1007/s10162-011-0311-2

JARO
Journal of the Association for Research in Otolaryngology

Altered Phenotype of the Vestibular Organ in GLAST-1 Null Mice

Sebastian P. Schraven[1], Christoph Franz[1], Lukas Rüttiger[1], Hubert Löwenheim[2], Anna Lysakowski[3], Wilhelm Stoffel[4], and Marlies Knipper[1]

[1]*Department of Otolaryngology, Tübingen Hearing Research Centre (THRC), Molecular Physiology of Hearing, University of Tübingen, Elfriede-Aulhorn-Str. 5, 72076 Tübingen, Germany*

[2]*Department of Otolaryngology, Tübingen Hearing Research Centre (THRC), Regenerative Biology, University of Tübingen, Elfriede-Aulhorn-Str. 5, 72076 Tübingen, Germany*

[3]*Department of Anatomy and Cell Biology, College of Medicine, University of Illinois at Chicago (UIC), 808 S. Wood St., Chicago, IL 60612, USA*

[4]*Laboratory of Molecular Neuroscience, Faculty of Medicine, Centre of Molecular Medicine, Cologne (CMMC) and Cluster of Excellence: Cellular Stress Responses in Aging-Associated Diseases, Cologne (CECAD); Institute of Biochemistry, University of Cologne, Zülpicher Str. 47a, 50674 Cologne, Germany*

Received: 4 April 2011; Accepted: 21 December 2011; Online publication: 14 February 2012

ABSTRACT

Various studies point to a crucial role of the high-affinity sodium-coupled glutamate aspartate transporter GLAST-1 for modulation of excitatory transmission as shown in the retina and the CNS. While 2–4-month-old GLAST-1 null mice did not show any functional vestibular abnormality, we observed profound circling behavior in older (7 months) animals lacking GLAST-1. An unchanged total number of otoferlin-positive vestibular hair cells (VHCs), similar ribbon numbers in VHCs, and an unchanged VGLUT3 expression in type II VHCs were detected in GLAST-1 null compared to wild-type mice. A partial loss of supporting cells and an apparent decline of a voltage-gated channel potassium subunit (KCNQ4) was observed in postsynaptic calyceal afferents contacting type I VHCs, together with a reduction of neurofilament- (NF200-) and vesicular glutamate transporter 1- (VGLUT1-) positive calyces in GLAST-1 null mice. Taken together, GLAST-1 deletion appeared to preferentially affect the maintenance of a normal postsynaptic/neuronal phenotype, evident only with increasing age.

Keywords: GLAST-1, vestibular hair cells, supporting cells, otoferlin, KCNQ4, VGLUT

Abbreviations: GLAST-1 – glutamate aspartate transporter 1; VGLUT – vesicular glutamate transporter; VHCs – vestibular hair cells; SCs – supporting cells; WT – wild-type; *sm* – saccular macula; *um* – utricular macula; *ca* – *cristae ampullares*; IHCs – inner hair cells; OHCs – outer hair cells; CNS – central nervous system

INTRODUCTION

In excitatory synapses the glutamate aspartate transporter 1 (GLAST-1) plays an important role by limiting the accumulation of extracellular glutamate to avoid excitotoxic cell damage (Storck et al. 1992; Klockner et al. 1993, 1994; Wahle and Stoffel 1996; Peghini et al. 1997; Danbolt 2001; Stoffel et al. 2004; Koeberle and Bahr 2008). In the CNS, GLAST-1 is expressed predominantly by glial cells, of which astrocyte glia have the highest density of GLAST-1 membrane expression (Storck et al. 1992; Rothstein et al. 1994). In glial cells,

Sebastian P. Schraven and Christoph Franz are joint first authors.

Correspondence to: Marlies Knipper · Department of Otolaryngology, Tübingen Hearing Research Centre (THRC), Molecular Physiology of Hearing · University of Tübingen · Elfriede-Aulhorn-Str. 5, 72076 Tübingen, Germany. Telephone: +49-7071-2988244; fax: +49-7071-294950; email: marlies.knipper@uni-tuebingen.de

GLAST-1 has been described as playing an important role in the termination of neurotransmitter signals (Storck et al. 1992; Lehre and Danbolt 1998). In retinal glia-type Müller cells, GLAST-1 function has been extensively analyzed (for review, see Bringmann et al. 2009). GLAST-1 was hypothesized to play a crucial role for termination of retinal signal transmission at the level of photoreceptor cells and bipolar cells, leading to a reduced b-wave and decreased oscillatory potentials in electroretinography when GLAST-1 is deleted (Harada et al. 1998). In the inner ear, the role of GLAST-1 is poorly understood. In the mammalian cochlea, supporting cells surrounding the inner hair cells (IHCs) exhibit intense labeling of GLAST-1, while Deiter's cells show weak immunoreactivity (Furness and Lehre 1997; Furness and Lawton 2003). An increased accumulation of glutamate in the perilymph after noise overstimulation has been described in GLAST-1 null mice, resulting in exacerbation of hearing loss (Hakuba et al. 2000). In the vestibular end organ, where glutamate release conveys acceleration and positioning information to the CNS via vestibular hair cells (VHCs; Matsubara et al. 1999; Bonsacquet et al. 2006), GLAST-1 has been shown in the plasma membranes of vestibular peripheral supporting cells (Takumi et al. 1997).

Previous studies analyzing 2–4-month-old GLAST-1 null mice observed no conspicuously abnormal motor activity or behavior (Watase et al. 1998; Stoffel et al. 2004). In this study, we analyzed older (7 month-old) GLAST-1 null mice and observed striking circling behavior in GLAST-1 null mice, but not in age-matched WT controls, which motivated us to perform a detailed immunohistochemical study of the vestibular organ in GLAST-1 null mice. Using hair cell and neuronal markers, a vestibular phenotype is described that points to a crucial function of GLAST-1 for maintenance of normal vestibular function.

METHODS

Animals

Six wild-type (WT) and five GLAST-1 null mice, aged 7 months, were used in this study. The WT and null mice analyzed here were bred in a CD1 outbreed background and they differed from the previously investigated WT and GLAST-1 null mice, described by Stoffel et al. (2004), that were bred on a C57Bl/6 background. Animal experiments were approved by and complied with all protocol requirements of the University of Tübingen.

Tissue preparation

WT and GLAST-1 null mice were deeply anesthetized (CO_2) followed by decapitation. The temporal bones containing the inner ear were dissected, fixed, and cryo-sectioned as previously described (Knipper et al. 2000). Briefly, temporal bones were fixed by immersion in 2% paraformaldehyde (all chemicals from SIGMA-Aldrich, Munich, Germany, unless stated otherwise), 125 mM sucrose in 100 mM phosphate-buffered saline (PBS, pH 7.4), for 2 h and decalcified (RDO, Apex Engineering Products Corporation, Aurora, Illinois, USA) for 45 min followed by overnight incubation in 25% sucrose in HEPES-Hanks solution, pH 7.4. Temporal bones were embedded in Tissue-Tek compound (Sakura Finetek Europe, Zoeterwoude, The Netherlands), cryo-sectioned at 10 µm, mounted on SuperFrost*/plus microscope slides, dried for 1 h, and stored at −20°C before use.

Light microscopy and fluorescence immunohistochemistry

The cationic dye toluidine blue was used to visualize the morphology of the cryo-sectioned vestibular organs. For immunohistochemistry, sections were stained and imaged as previously described (Knipper et al. 2000). Briefly, sections were thawed and permeabilised with 0.5% Triton X-100 for 10 min at room temperature, blocked with 4% normal goat serum (NGS) in 1× PBS, and incubated with primary antibody in 1% NGS in 1× PBS containing 0.1% Triton X-100 overnight at 4°C. Rabbit polyclonal antibodies against GLAST-1 (1:50; Storck et al. 1992), otoferlin (1:6,000; Schug et al. 2006), KCNQ4 (1:50; Ruttiger et al. 2004; Winter et al. 2006), VGLUT2 (1:100; Synaptic Systems, Göttingen, Germany) and VGLUT3 (1:300; Synaptic Systems), mouse monoclonal antibodies against otoferlin (1:50; Abcam, Cambridge, UK), neurofilament NF200 (1:10,000; SIGMA-Aldrich), VAMP2 (1:50; Synaptic Systems) anti-CtBP2/RIBEYE (1:50; BD Transduction Laboratories, CA, USA), and guinea pig polyclonal antibodies against VGLUT1 (1:250; Synaptic Systems) were used. Primary antibodies were visualized with either Cy3-conjugated goat anti-rabbit (1:1,500; Jackson Immuno Research Laboratories, West Grove, PA, USA), Alexa-488-conjugated goat anti-mouse antibodies (1:500; Molecular Probes, Leiden, The Netherlands), or with Alexa-488-conjugated goat anti-guinea pig antibodies (1:500; Sigma Molecular Probes). Sections were rinsed and mounted in Vectashield mounting medium containing the nuclear marker DAPI (Vector Laboratories, Burlingame, CA, USA). For all immunoreactions, negative controls (only secondary antibody incubation) were also included, the confirmation of GLAST-1 antibody specificity was analyzed in sections of GLAST-1 null mice. Sections were viewed using an upright Olympus

BX61 microscope equipped with motorized *z*-axis, bright field and epifluorescence illumination and differential interference contrast (DIC). Images were acquired using a CCD camera and analyzed with cellSens Dimension software (OSIS, Münster, Germany). An overview of the vestibular system (Fig. 2) is composed of images aligned using the multiple image alignment tool (MIA, OSIS). For fluorescence microscopy, slices were imaged over a distance of several µm in an image-stack along the *z*-axis (*z*-stack) followed by three-dimensional deconvolution using cellSens Dimension module with the advanced maximum likelihood estimation algorithm (ADVMLE, OSIS) in order to increase spatial resolution and to minimize background haze. Figures 3, 4, 5, 6, and 7 show composite images of such deconvoluted *z*-stacks, which represent maximum intensity projections over all layers of the *z*-stack. Images were processed with Photoshop.

Statistical analyses

To estimate the ratio of VHCs (stained by otoferlin) and KCNQ4-positive type I VHCs in the saccular (*sm*) and utricular maculae (*um*) as well as cristae ampullares (*ca*) epithelia of GLAST-1 null mice, DAPI-stained nuclei of otoferlin- and KCNQ4-positive cells were counted for at least 3 different slices of 5 null and 6 WT mice and normalized to the numbers in WT mice. Mean values and standard deviation are listed. For evaluation of the number of ribbons per VHC in WT and GLAST-1 null mice, CtBP2-positive ribbon structures of 15 VHCs were counted in cross-sections of the sensory epithelia, using image stacks of the *um* and taking the position of DAPI-stained nuclei as an indicator for mainly VHCs. No special differentiation between type I and type II VHCs and supporting cells that might be at the hair cell level has been performed. Immunochemical stainings and cell counts were replicated for at least 3 different slices of 3 different mice per genotype. For statistical analyses, unpaired Student's *t* test was performed to compare variances of the data obtained from counting. Differences were considered statistically significant for p values <0.05.

RESULTS

Since the first description of GLAST-1 null mice at 2–4 months of age, in which no circling behavior was apparent (Storck et al. 1992), no attention has been given to older stages. We observed obvious late onset severe circling behavior in all five 7-month-old GLAST-1 null mice (Fig. 1). GLAST-1 null mice started circling at around 5 months of age. Although circling in GLAST-1 null mice (n=5) occurred at an approximate frequency of 60 to 70 circles per minute, no directional preference was observed. We did not attempt to perform any behavioral or coordination tests to assess vestibular function since it has been observed by Prof. W. Stoffel's lab that this test was not practical in GLAST-1 null mice at older ages due to their profound circling behavior. However, similar aged WT animals showed normal motor behavior.

Gross anatomical changes in vestibular organ of GLAST-1 null mice

Using toluidine blue staining, we compared the morphology of the vestibular sensory epithelia, i.e., saccular (*sm*) and utricular maculae (*um*) as well as cristae ampullares (*ca*) of WT (Fig. 2A, B) and GLAST-1 null mice (Fig. 2C). While vestibular epithelia appeared normal in WT mice (Fig. 2B), large cavities with diameters of 10–30 µm within the sensory epithelia were observed in 4 out of 5 GLAST-1 null mice shown exemplified for the utricular macula (Fig. 2C).

GLAST-1 deletion appears not to have a primary effect on VHCs

To specify whether circling behavior was due to the loss of VHCs or neuronal projection, we performed immunohistochemical investigations using marker proteins for hair cells. Otoferlin is a protein expressed in type I and type II VHCs (Dulon et al. 2009). Double-labeling with GLAST-1 (Fig. 3B) and otoferlin-specific antibodies (Fig. 3E) confirmed the staining pattern of GLAST-1 in supporting cells of all three vestibular sensory epithelia (*sm*, *um*, *ca*) as described by

FIG. 1. Circling behavior in GLAST-1 null mice. Mice lacking GLAST-1 show profound circling behavior with a frequency of 60–70 cycles per minute, as indicated by consecutive images taken over 1 s.

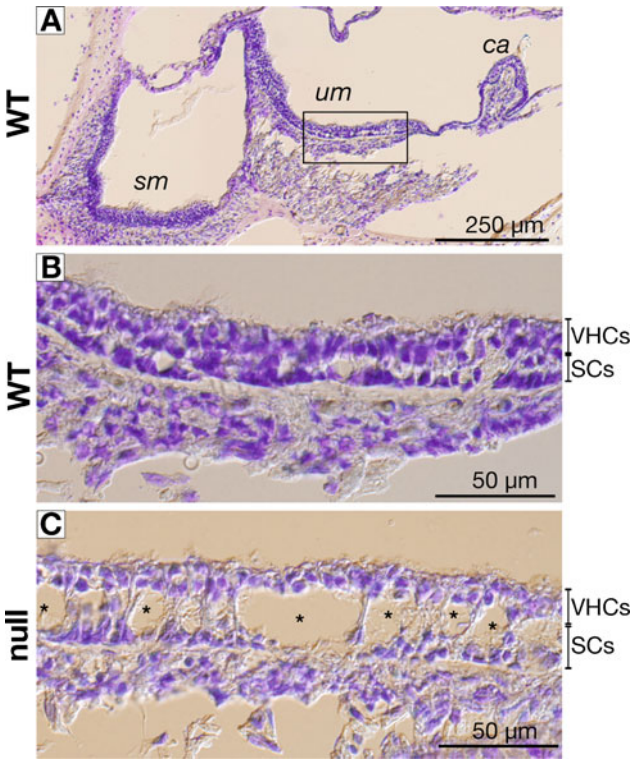

FIG. 2. Comparison of toluidine blue-stained vestibular sensory epithelia of wild-type (*WT*) and GLAST-1 null mice. **A** The vestibular organ is composed of the saccular macula (*sm*), the utricular macula (*um*), and the cristae ampullares (*ca*). **B** In WT mice, the vestibular epithelium, composed of mostly sensory cell nuclei with an underlying layer of supporting cell nuclei, appeared normal, exemplified for the *um*. In GLAST-1 null mice, large cavities (Ø=10–30 µm; *asterisks*) were observed within the supporting cell layer (**C**).

Takumi et al. (1997) and the absence of GLAST-1 in GLAST-1 null mice, exemplified for *sm* (Fig. 3A, D). GLAST-1 was not colocalized with the VHC marker otoferlin (Fig. 3C). Cell counts in *um* and *sm* were performed. When the number of otoferlin-positive cells was compared between WT (Fig. 4A, D) and null mice (Fig. 4B, C, E, F), there was no difference in VHC counts in *sm* and *um* of 5 of 5 GLAST-1 null mice. This quantification was based on counting DAPI-stained nuclei of otoferlin-positive cells in cross sectioned vestibular organs (Fig. 4G). The proportion of cell nuclei did not differ significantly for the *sm* (WT, 80.29±14.89 (n=6) vs. null, 76.75±13.1 (n=5); p>0.05), the *um* (WT, 74.67±7.0 (n=6) vs. null, 76.67±7.05 (n=5); p>0.05) as well as for the *ca* (WT, 45.82±6.29 (n=6) vs. null, 44.91±7.57 (n=5); p>0.05). This finding is further supported by an unaltered number of synaptic release sites per VHC (stained by CtBP2/RIBEYE, Fig. 5) in GLAST-1 null mice when compared to WT animals (n=3; WT, 2.46±0.32 vs. null, 2.57±0.42).

In conclusion, although the general morphology of the vestibular epithelia was altered, the data support the notion that these changes are not related to a primary effect on VHC phenotype.

GLAST-1 deletion appears to cause deterioration of the post-synaptic neuronal fibers

KCNQ4, a voltage-activated potassium channel that is also present in cochlear hair cells and spiral ganglia neurons, is preferentially expressed in the calyces surrounding type I VHCs (Hurley et al. 2006; Lysakowski et al. 2011), although KCNQ4 has been shown to be expressed in immature VHCs (Kharkovets et al. 2000; Sousa et al. 2009). In agreement with this, KCNQ4 protein staining in WT mice resembled NF200-positive staining in calyces surrounding type I VHCs in all vestibular sensory epithelia, as shown in Figure 6 (A, B) for *sm*. KCNQ4 and NF200 colocalized throughout the calyces ensheathing type I VHCs (Fig. 6C, asterisks). In GLAST-1 null mice, NF200 expression seemed to be reduced, accompanied by an altered appearance of the calyces as well as by a different appearance of NF200-positive fibers, especially in the region of supporting cells (Fig. 6D–F). GLAST-1 null mice also showed a strong reduction of KCNQ4 in the vestibular sensory epithelia (Fig. 6E). Coexpression of KCNQ4 and NF200 revealed a significant reduction of KCNQ4-labeled NF200-positive calyces (Fig. 6F, H, asterisks) in GLAST-1 null mice, suggesting that KCNQ4 loss may precede the loss of NF200-positive

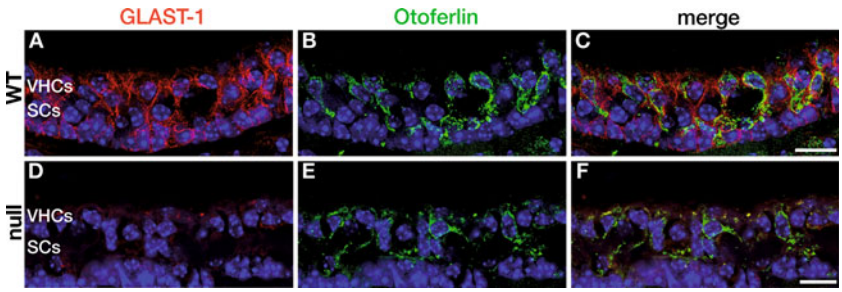

FIG. 3. GLAST-1 protein labeling in vestibular sensory epithelia of adult mice. **A–C** In wild-type animals (*WT*) using an anti-GLAST-1 antibody (*red*), protein expression was detected in cells that were not labeled by the vestibular hair cell marker otoferlin (*green*, merged images shown in **C**) as shown in the saccular macular (*sm*). **D–F** In GLAST-1 null mice no antibody signal was detected, otoferlin staining was not affected (merged images shown in **F**). Nuclear marker: DAPI (*blue*). *Scale bars* indicate 20 µm.

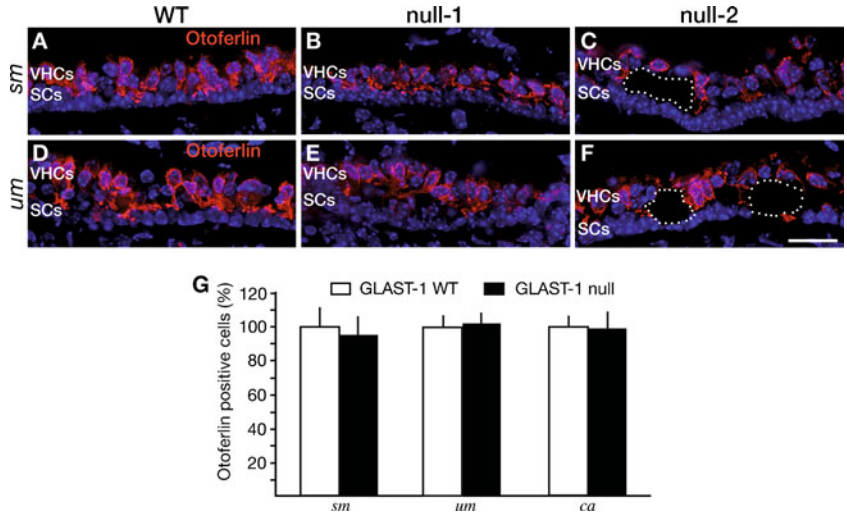

FIG. 4. Numbers of otoferlin-positive vestibular hair cells are unchanged in the absence of GLAST-1. Otoferlin protein is comparably expressed in VHCs of WT (**A**, **D**) and GLAST-1 null mice (**B**, **C**, **E**, **F**) in the saccular (*sm*) and utricular maculae (*um*). **B**, **E** In one (null-1) out of five 7-month-old GLAST-1 null mice investigated, no formation of large cavities was observed. **C**, **F** The remaining four GLAST-1 null mice all showed cavities (*dotted lines*) in the VHC layer (for example, null-2). **G** Statistical analyses of cell counts for otoferlin-positive VHCs in WT (n=6 animals; *white bars*) and GLAST-1 null mice (n=5 animals; *black bars*) in the *sm*, the *um*, and the cristae ampullares (*ca*). The proportion of otoferlin-positive cells reveals no difference in total numbers of vestibular hair cells between WT and GLAST-1 null mice (*sm*, 95.59%; *um*, 102.68%; *ca*, 98.01%). Nuclear marker: DAPI (*blue*). *Scale bar* indicates 20 μm.

calyces. This reduction was quantified as ~85% in the *sm* (WT, 69.58±5.82 (n=6) vs. null, 10.08±5.09 (n=5); p<0.001), ~77% in the *um* (WT, 70.67±4.08 (n=6) vs. null, 16.11±4.20 (n=5); p<0.001) as well as ~50% in the *ca* (WT, 74.80±6.11 (n=6) vs. null, 37.91± 9.45 (n=5); p<0.001; Fig. 6I).

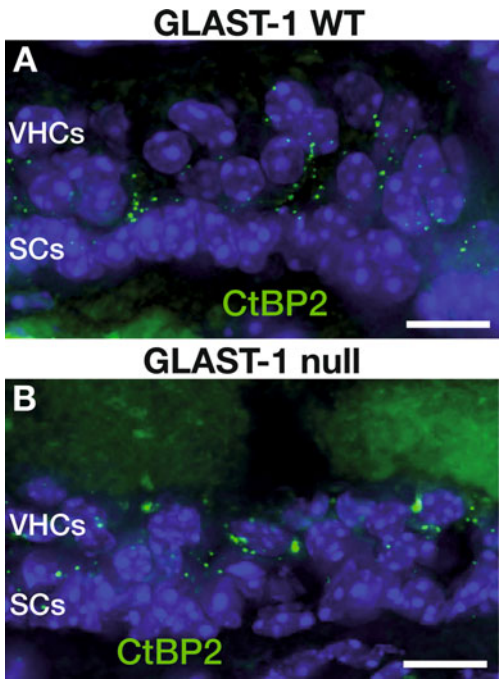

FIG. 5. Number of ribbon synapses in VHCs is unaltered in GLAST-1 null mice. The CtBP2/RIBEYE protein expression pattern is similar in WT (**A**) and GLAST-1 null mice (**B**). Nuclear marker: DAPI (*blue*). *Scale bars* indicate 10 μm.

To determine if the phenotype of hair cells and neurons is secondarily affected by the GLAST-1 deletion, we assessed the expression of vesicular glutamate transporters (VGLUTs) 1–3, which are known to mirror the aspect of metabolically demanding vesicular transport (Heidrych et al. 2009) and whose expression has been reported recently in vestibular sensory epithelia (Zhang et al. 2010). We observed VGLUT1 labeling in NF200-positive fibers and calyces (Fig. 7A–D) that was similarly reduced as NF200 labeling in GLAST-1 null mice (Fig. 6).

VGLUT3 has been described as a marker for synaptic vesicular trafficking (Heidrych et al. 2009). VGLUT3 staining in vestibular sensory epithelia of GLAST-1 deficient and control mice did not colocalize with NF200 labeling, but instead, intensively labeled calyx free VHCs (Fig. 7E–H), indicating that VGLUT3 is a marker for type II, rather than type I, VHCs. The deletion of GLAST-1 had no obvious effect on VGLUT3 labeling.

Staining of vestibular sensory epithelia for VGLUT2 (Fig. 7I, J) displayed almost no colocalization with NF200 labeling in afferent fibers of type I VHCs (Fig. 7I, J) but a pronounced labeling of unclear origin was observed at the apical neck region of VHCs. To disclose the nature of VGLUT2 labeling at the VHC's apex, colabeling using VAMP2 (a marker for cochlear efferent fibers, see Safieddine and Wenthold 1999), was performed in WT animals. VAMP2 colocalizes with VGLUT2 labeling indicating presumptive efferent projections onto the apical neck region of VHCs (Fig. 7I, J).

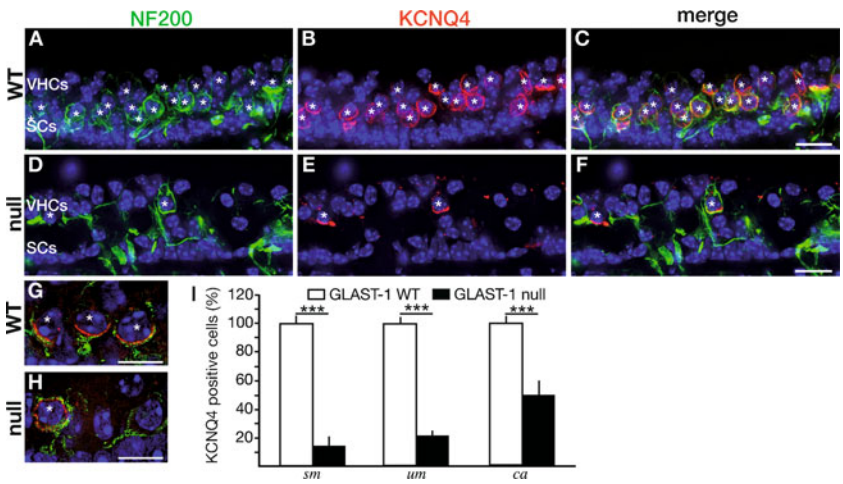

FIG. 6. Vestibular calyces are strongly affected by loss of GLAST-1. **A**, **D** Anti-Neurofilament 200 (NF200, *green*) antibody, a marker for afferents innervating type I VHCs, labeled calyces of type I VHCs of WT and GLAST-1 null mice, shown here for the saccular macula (*sm*). In GLAST-1 null mice NF200 protein expression appeared altered in comparison to WT. **B**, **E** KCNQ4 protein (*red*) was heavily expressed in NF200-positive calyces surrounding WT type I VHCs (merged images shown in **C**, magnified example in **G**). In GLAST-1 null mice, KCNQ4 protein expression was strongly reduced revealing a heterogeneous pattern of few calyces positive for KCNQ4 and NF200, in addition to NF200-positive calyces without KCNQ4 staining (merged images shown in **F**, magnified example in **H**). **I** Statistical analyses of counts for KCNQ4-positive calyces in WT (n=6; *white bars*) and GLAST-1 null mice (n=5; *black bars*) in the *sm*, the utricular macula (*um*), and the cristae ampullares (*ca*). The proportion of KCNQ4-positive calyces is significantly reduced in GLAST-1 null mice (*sm*, 14.49%; *um*, 22.80%; *ca*, 50.68%; ***p<0.001). Nuclear marker: DAPI (*blue*). *Asterisks* indicate NF200- and KCNQ4-positive type I VHCs. *Scale bars* in **A**–**F** indicate 20 µm; *scale bars* in **G** and **H** indicate 5 µm.

This staining pattern was unaltered in absence of GLAST-1 (Fig. 7K–N), which may challenge the presumption that the GLAST-1 deletion primarily affects afferent, rather than efferent, fibers or VHCs. We cannot exclude, however, that in addition to NF200-positive calyceal afferent fibers contacting type I VHCs, also afferent fibers contacting type II VHCs may be affected.

In summary, the GLAST-1 deletion in aged animals was observed to lead to reduced expression of KCNQ4, VGLUT1, and NF200 in calyceal endings, as well as to an altered appearance of remaining NF200-positive calyces and fibers. The deletion did not affect the expression of VGLUT3 and VGLUT2. Interestingly, VGLUT2 was found at VAMP2-positive structures close to the apex of VHCs.

DISCUSSION

Loss of GLAST-1 leads to a late onset circling behavior

In the mouse vestibular epithelia, both type I and type II VHCs release glutamate as a transmitter (Altschuler et al. 1989; Usami et al. 1992; Usami and Ottersen 1995), and GLAST-1 has been shown to be the major glutamate transporter used for clearance of glutamate from the synaptic cleft, in supporting cells surrounding both VHC types (Takumi et al. 1997) thereby preventing excitotoxic effects. In contrast to previous studies that analyzed young GLAST-1 null mice without any obvious vestibular phenotype (Rothstein et al. 1996; Harada et al. 1998; Watanabe et al. 1999; Hakuba et al. 2000; Tsuru et al. 2002; Stoffel et al. 2004; Sarthy et al. 2005; Shimizu et al. 2005; Matsugami et al. 2006; Harada et al. 2007; Takasaki et al. 2008; Karlsson et al. 2009), we demonstrate a profound circling behavior in aged (7-month-old) GLAST-1 null mice suggesting a late onset or progression of an altered vestibular phenotype. However, it remains

FIG. 7. Expression of VGLUT1-3 in the adult vestibular system of GLAST-1 null mice. In WT animals (**A**, boxed area enlarged in **B**), VGLUT1 (*green*, *arrowheads*) was predominantly expressed in NF200-positive calyces (*red*, *arrowheads*) surrounding type I VHCs (*yellow* indicates colocalization), mainly in the central zone as shown here in the crista ampullaris. VGLUT1 labeling in GLAST-1 null mice showed deterioration similar to NF200 expression (**C**, boxed area enlarged in **D**). VGLUT3 expression (*red*, *open arrowheads*) of WT (**E**, boxed area enlarged in **F**) and null mice (**G**, boxed area enlarged in **H**) resembles expression in type II VHCs, but not type I VHCs, as indicated by the absence of VGLUT3 from NF200-positive calyces (*green*, *arrowheads*). GLAST-1 null mice showed no obvious reduction in VGLUT3 signal. VGLUT3 was predominantly expressed in the peripheral zone. VGLUT2 immunohistochemistry in WT (**I**, boxed area enlarged in **J**) and GLAST-1 null mice (**K**, boxed area enlarged in **L**) revealed VGLUT2-positive contacts (*red*, *arrows*) at the apical neck region of type I and type II VHCs. Almost no colocalization of VGLUT2 with the calyx afferent fiber marker NF200 (*green*, *arrowheads*) could be detected. In addition, VGLUT2 (*red*, *arrows*) was colocalized with the vesicle-associated membrane protein-2 (VAMP2, *green*, *arrows*), a marker for presynaptic efferent contacts in the cochlea (**M**, boxed area enlarged in **N**; *yellow* indicates colocalization). Nuclear marker: DAPI (*blue*). **A**, **C**, **E**, **G**, **I**, **K**, and **M** superimposed with DIC image. *Scale bars* in **A**, **C**, **E**, **G**, **I**, **K**, and **M** are 20 µm, and in **B**, **D**, **F**, **H**, **J**, **L**, and **N** are 10 µm.

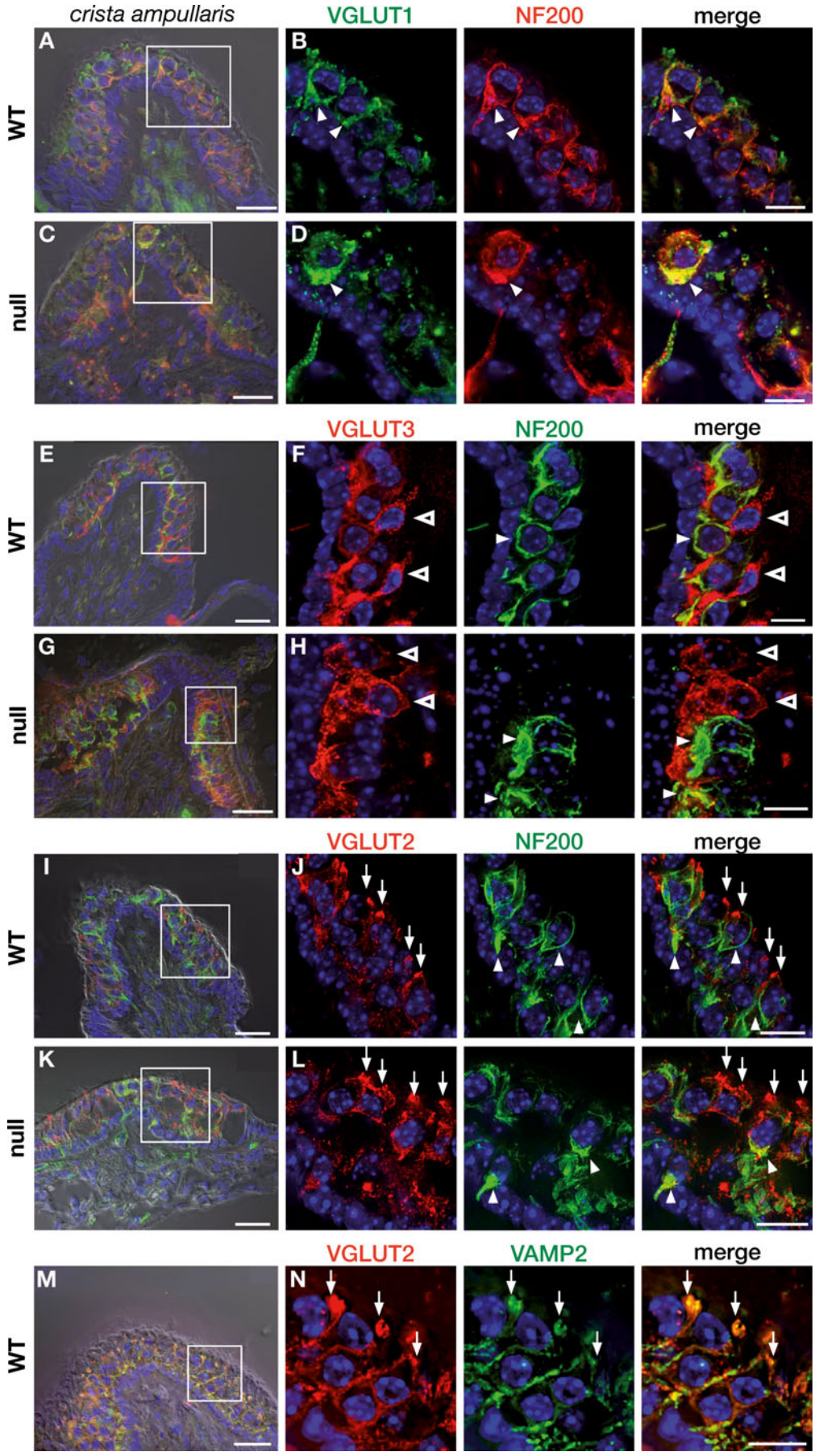
crista ampullaris
VGLUT1
NF200
merge
A
B
WT
C
D
null
VGLUT3
NF200
merge
E
F
WT
G
H
null
VGLUT2
NF200
merge
I
J
WT
K
L
null
VGLUT2
VAMP2
merge
M
N
WT

unclear to what extent each of the five affected vestibular sensory epithelia contributes to the observed phenotype.

Loss of GLAST-1 results in distinctive changes in the vestibular sensory epithelia

Our data confirm previous findings, which show that GLAST-1 is not present in type I and II VHCs, but rather in the surrounding supporting cells (Takumi et al. 1997). The observed unaltered number of ribbons in the vestibular sensory epithelia in the mutant animals compared to WT controls points to unaffected pre-synaptic sites (Fig. 5). However, in the literature, 20–25 ribbons in type I and about 15 ribbons in type II VHCs have been found in chinchilla vestibular system (Lysakowski and Goldberg 1997). To our knowledge, the only study on the number of ribbons in the VHCs of mice currently available is in postnatal developing ICR mice (Lysakowski 1999). The low number in the present study could be related to strain differences and/or methodological counting differences. As WT animals had similar low ribbon counts and yet showed no disturbed vestibular function we also may consider an age-related effect as to the knowledge of the authors the ribbon number of VHCs of mice older than postnatal Day 28 has not been investigated.

The cavities observed within the vestibular sensory epithelia were found in four of five GLAST-1 null mice (Fig. 2). Why this phenotype was not expressed in the one of these five animals even though all were the same age (7 months) remains unclear. One may speculate about intra-species differences leading to a different progression of cavity formation. However, in the animal with normal vestibular morphology, circling behavior and all other immunohistochemically observed differences were similar to those observed in the other four GLAST-1 null mice.

Therefore, the cavities, in addition to preservation of VHCs (Fig. 4), may indicate that supporting cells, rather than VHCs, are degenerating in the absence of GLAST-1. It is assumed that with the loss of supporting cells, their metabolic functions in relation to sensory cells and afferent projections is affected, as well as their function in glutamate clearance from the synaptic region by glutamate uptake through GLAST-1 (Kim et al. 2010). The latter affects predominantly calyceal endings at the age investigated. Furthermore, type I VHCs have more synaptic ribbons (Lysakowski and Goldberg 1997) and therefore it is likely that more glutamate is released into the synaptic cleft of the calyx upon depolarization, which in the absence of GLAST-1 accumulates with little ability to leave the cleft by diffusion. Therefore, we may speculate that calyces innervating type I VHCs are more affected or are affected earlier than bouton synapses on type II VHCs. The assumed hyper-excitation of post-synaptic calyces may be causally involved in the observed loss of KCNQ4 from NF200-positive calyces. So far, KCNQ4 has been reported in IHCs (Oliver et al. 2003), outer hair cells (OHCs; Kharkovets et al. 2000), vestibular calyces (Lysakowski et al. 2011), as well as in VHCs (Rocha-Sanchez et al. 2007). With our antibody, however, we did not observe KCNQ4 labeling in type II VHCs, as described by Rocha-Sanchez et al. (2007). KCNQ4 carries K^+ outflow of cells, thereby it sets the resting membrane potential of inner ear hair cells thus

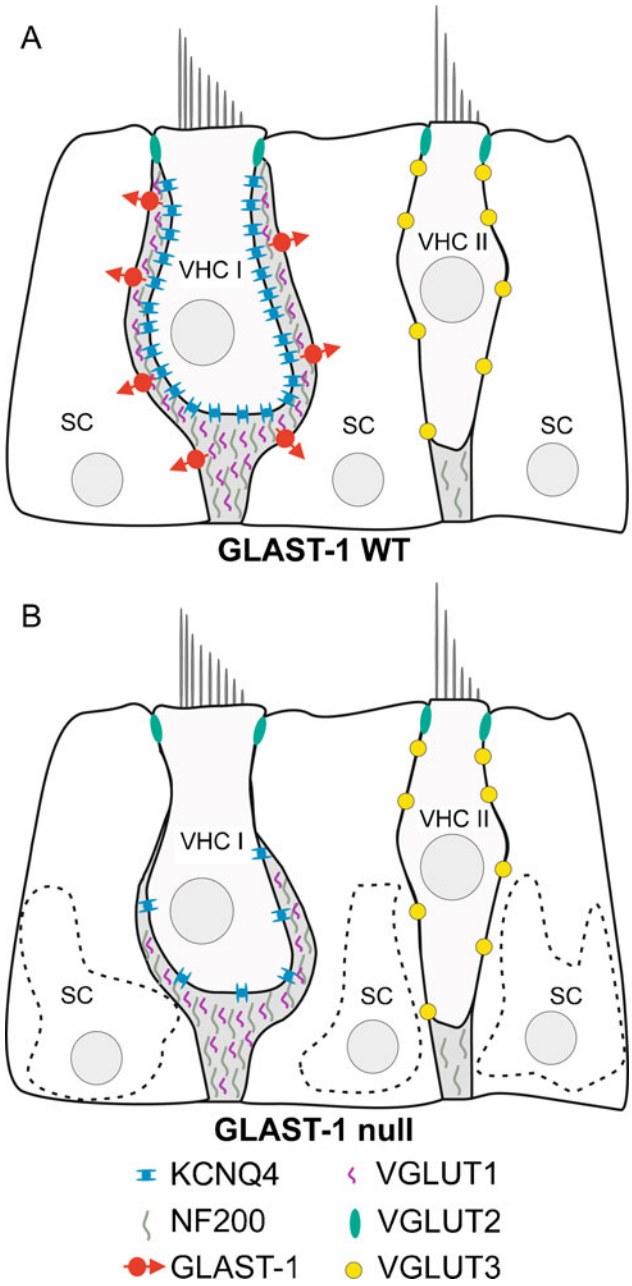

FIG. 8. Schematic illustration of GLAST-1, KCNQ4, NF200 and VGLUT1-3 expression in the vestibular sensory epithelia of WT (**A**) and GLAST-1 null mice (**B**). *SC,* supporting cell; *VHC I,* type I vestibular hair cell; *VHC II,* type II vestibular hair cell.

maintaining intracellular Ca^{2+} concentration at low levels (Oliver et al. 2003). The loss or decline of KCNQ4 channel results in progressive degeneration of IHC synapses (Oliver et al. 2003) as well as OHC synapses (Ruttiger et al. 2004) resulting in progressive hearing loss (Kubisch et al. 1999). We hypothesize that a loss of KCNQ4 in afferent calyces, following sustained hyper-excitation by impaired glutamate clearance from the synaptic cleft, might be causally related to the observed decline of vestibular calyx afferent fibers in GLAST-1 deficient mice. High-resolution studies using electron microscopy are needed to clarify this aspect and also to clarify the extent to which bouton synapses of type II VHCs are affected or not in GLAST-1 null mice. One may also raise the question of whether the reduction of calyceal afferent endings is perhaps secondary to a loss of ribbon synapses. In cochlear IHCs, the loss of ribbons has been reported to occur secondarily to the loss of afferent fibers (Kujawa and Liberman 2009). So far, however, to the authors' knowledge, which effect is primary and which secondary has not yet been clarified for the vestibular system. Interestingly, in light of our data, humans carrying a mutation in the KCNQ4 gene, which causes a dominant autosomal hearing disorder (DFNA2), also exhibit vestibular dysfunction (De Leenheer et al. 2002), a finding so far not described in animal models in the literature. It would be interesting to analyze whether a late onset vestibular phenotype also occurs in KCNQ4-deficient mice.

We intended to get more insight into presumptive additional consequences of GLAST-1 deletion for presynaptic function by investigating the expression of VGLUT1-3, which have recently been shown to be present in the rat vestibular system (Zhang et al. 2010). VGLUTs are known to be crucial for reuptake of glutamate into vesicles of presynapses (Takamori et al. 2000) and mirror disturbed vesicle trafficking (Heidrych et al. 2009).

Both afferent VGLUT1 (Fig. 8) and NF200 (Fig. 8) showed similar reductions in the vestibular sensory epithelia of GLAST-1 null mice. However, KCNQ4 expression (Fig. 8) seemed to be affected to a greater extent, since the number of NF200-positive calyces without KCNQ4 staining in GLAST-1 null mice was higher than the number of calyces positive for both. Although currently shown only on a qualitative level, data point to a primary effect of GLAST-1 deletion on calyx endings, in which KCNQ4 loss precedes loss of NF200 and VGLUT1. Accordingly, the loss of KCNQ4 expression following GLAST-1 deletion may occur in the vestibular organ, similar to that previously described in the cochlea (Hakuba et al. 2000) and in the retina (Park et al. 2009; Harada et al. 2010).

In contrast to previous studies (Zhang et al. 2010), we did not observe colocalization of VGLUT1 and VGLUT3 in 7-month-old mouse VHCs, but we demonstrated a differential expression pattern, with VGLUT1 expressed in calyx-bearing afferents, predominantly in the striola (Desai et al. 2005), and VGLUT3 expressed in type II VHCs, more numerous in the extrastriola (Desai et al. 2005). Less clear is the supranuclear pattern found for VGLUT2 in type I and type II VHCs, pointing to a presynaptic localization as assumed by colocalization with the efferent marker VAMP2. We cannot completely exclude VGLUT1 expression in VHCs, however high resolution studies, e.g., transmission electron microscopy, are required to distinguish VGLUT1, VGLUT2, and VGLUT3 expression in calyces vs. epithelial cells.

The similarity of altered NF200 and VGLUT1 staining in GLAST-1 null mice, with no obvious differences in VGLUT2 (in efferents or VHCs) and VGLUT3 (presumptive marker for type II VHCs), strengthen the hypothesis that GLAST-1 deletion preferentially affects the synaptic structures of type I VHCs.

In conclusion, our data suggest that the loss of GLAST-1 in supporting cells and the subsequent loss of supporting cells in vestibular sensory epithelia causes a late onset vestibular phenotype, mainly affecting calyx-bearing afferent fibers (presumably by excitotoxic accumulation of glutamate), which in turn leads to reduced KCNQ4, NF200, and VGLUT1 expression. This phenotype coincides with the development of circling behavior in aged GLAST-1 null mice and might lead to vestibular dysfunction. Our findings point to a pivotal role of GLAST-1 for preserving sensory function not only in the vestibular system but also in the cochlea (Hakuba et al. 2000) and the retina (Park et al. 2009; Harada et al. 2010).

ACKNOWLEDGMENTS

The authors would like to thank Karin Rohbock and Barbara Holz for technical assistance. S.P.S., C.F., L.R., H.L., and M.K. supported by the European Commission, Marie Curie Training Site HEARING (QLG3-CT-2001-60009) and the Deutsche Forschungsgemeinschaft DFG Kni 316/4-3; A.L. supported by NIH R01 DC 02058; W.S. supported by the Centre of Molecular Medicine, University of Cologne (CMMC) and the Cluster of Excellence: Cellular Stress Responses in Aging-Associated Diseases, University of Cologne (CECAD).

REFERENCES

ALTSCHULER RA, SHERIDAN CE, HORN JW, WENTHOLD RJ (1989) Immunocytochemical localization of glutamate immunoreactivity in the guinea pig cochlea. Hear Res 42:167–173

BONSACQUET J, BRUGEAUD A, COMPAN V, DESMADRYL G, CHABBERT C (2006) AMPA type glutamate receptor mediates neurotransmission at turtle vestibular calyx synapse. J Physiol 576:63–71

BRINGMANN A, PANNICKE T, BIEDERMANN B, FRANCKE M, IANDIEV I, GROSCHE J, WIEDEMANN P, ALBRECHT J, REICHENBACH A (2009) Role of retinal glial cells in neurotransmitter uptake and metabolism. Neurochem Int 54:143–160

DANBOLT NC (2001) Glutamate uptake. Prog Neurobiol 65:1–105

DE LEENHEER EM, HUYGEN PL, COUCKE PJ, ADMIRAAL RJ, VAN CAMP G, CREMERS CW (2002) Longitudinal and cross-sectional phenotype analysis in a new, large Dutch DFNA2/KCNQ4 family. Ann Otol Rhinol Laryngol 111:267–274

DESAI SS, ZEH C, LYSAKOWSKI A (2005) Comparative morphology of rodent vestibular periphery. I. Saccular and utricular maculae. J Neurophysiol 93:251–266

DULON D, SAFIEDDINE S, JONES SM, PETIT C (2009) Otoferlin is critical for a highly sensitive and linear calcium-dependent exocytosis at vestibular hair cell ribbon synapses. J Neurosci 29:10474–10487

FURNESS DN, LAWTON DM (2003) Comparative distribution of glutamate transporters and receptors in relation to afferent innervation density in the mammalian cochlea. J Neurosci 23:11296–11304

FURNESS DN, LEHRE KP (1997) Immunocytochemical localization of a high-affinity glutamate–aspartate transporter, GLAST, in the rat and guinea-pig cochlea. Eur J Neurosci 9:1961–1969

HAKUBA N, KOGA K, GYO K, USAMI SI, TANAKA K (2000) Exacerbation of noise-induced hearing loss in mice lacking the glutamate transporter GLAST. J Neurosci 20:8750–8753

HARADA T, HARADA C, WATANABE M, INOUE Y, SAKAGAWA T, NAKAYAMA N, SASAKI S, OKUYAMA S, WATASE K, WADA K, TANAKA K (1998) Functions of the two glutamate transporters GLAST and GLT-1 in the retina. Proc Natl Acad Sci USA 95:4663–4666

HARADA T, HARADA C, NAKAMURA K, QUAH HM, OKUMURA A, NAMEKATA K, SAEKI T, AIHARA M, YOSHIDA H, MITANI A, TANAKA K (2007) The potential role of glutamate transporters in the pathogenesis of normal tension glaucoma. J Clin Invest 117:1763–1770

HARADA C, NAMEKATA K, GUO X, YOSHIDA H, MITAMURA Y, MATSUMOTO Y, TANAKA K, ICHIJO H, HARADA T (2010) ASK1 deficiency attenuates neural cell death in GLAST-deficient mice, a model of normal tension glaucoma. Cell Death Differ 17:1751–1759

HEIDRYCH P, ZIMMERMANN U, KUHN S, FRANZ C, ENGEL J, DUNCKER SV, HIRT B, PUSCH CM, RUTH P, PFISTER M, MARCOTTI W, BLIN N, KNIPPER M (2009) Otoferlin interacts with myosin VI: implications for maintenance of the basolateral synaptic structure of the inner hair cell. Hum Mol Genet 18:2779–2790

HURLEY KM, GABOYARD S, ZHONG M, PRICE SD, WOOLTORTON JR, LYSAKOWSKI A, EATOCK RA (2006) M-like K+currents in type I hair cells and calyx afferent endings of the developing rat utricle. J Neurosci 26:10253–10269

KARLSSON RM, TANAKA K, SAKSIDA LM, BUSSEY TJ, HEILIG M, HOLMES A (2009) Assessment of glutamate transporter GLAST (EAAT1)-deficient mice for phenotypes relevant to the negative and executive/cognitive symptoms of schizophrenia. Neuropsychopharmacology 34:1578–1589

KHARKOVETS T, HARDELIN JP, SAFIEDDINE S, SCHWEIZER M, EL-AMRAOUI A, PETIT C, JENTSCH TJ (2000) KCNQ4, a K+channel mutated in a form of dominant deafness, is expressed in the inner ear and the central auditory pathway. Proc Natl Acad Sci USA 97:4333–4338

KIM E, HYRC KL, SPECK J, LUNDBERG YW, SALLES FT, KACHAR B, GOLDBERG MP, WARCHOL ME, ORNITZ DM (2010) Regulation of cellular calcium in vestibular supporting cells by Otopetrin 1. J Neurophysiol 104:3439–3450

KLOCKNER U, STORCK T, CONRADT M, STOFFEL W (1993) Electrogenic L-glutamate uptake in Xenopus laevis oocytes expressing a cloned rat brain L-glutamate/L-aspartate transporter (GLAST-1). J Biol Chem 268:14594–14596

KLOCKNER U, STORCK T, CONRADT M, STOFFEL W (1994) Functional properties and substrate specificity of the cloned L-glutamate/L-aspartate transporter GLAST-1 from rat brain expressed in Xenopus oocytes. J Neurosci 14:5759–5765

KNIPPER M, ZINN C, MAIER H, PRAETORIUS M, ROHBOCK K, KOPSCHALL I, ZIMMERMANN U (2000) Thyroid hormone deficiency before the onset of hearing causes irreversible damage to peripheral and central auditory systems. J Neurophysiol 83:3101–3112

KOEBERLE PD, BAHR M (2008) The upregulation of GLAST-1 is an indirect antiapoptotic mechanism of GDNF and neurturin in the adult CNS. Cell Death Differ 15:471–483

KUBISCH C, SCHROEDER BC, FRIEDRICH T, LUTJOHANN B, EL-AMRAOUI A, MARLIN S, PETIT C, JENTSCH TJ (1999) KCNQ4, a novel potassium channel expressed in sensory outer hair cells, is mutated in dominant deafness. Cell 96:437–446

KUJAWA SG, LIBERMANN MC (2009) Adding insult to injury: cochlear nerve degeneration after "temporary" noise-induced hearing loss. J Neurosci 29:14077–14085

LEHRE KP, DANBOLT NC (1998) The number of glutamate transporter subtype molecules at glutamatergic synapses: chemical and stereological quantification in young adult rat brain. J Neurosci 18:8751–8757

LYSAKOWSKI A (1999) Development of synaptic innervation in the rodent utricle. Ann N Y Acad Sci 871:422–425

LYSAKOWSKI A, GOLDBERG JM (1997) A regional ultrastructural analysis of the cellular and synaptic architecture in the chinchilla cristae ampullares. J Comp Neurol 389:419–443

LYSAKOWSKI A, GABOYARD-NIAY S, CALIN-JAGEMAN I, CHATLANI S, PRICE SD, EATOCK RA (2011) Molecular microdomains in a sensory terminal, the vestibular calyx ending. J Neurosci: Off J Soc Neurosci 31:10101–10114

MATSUBARA A, TAKUMI Y, NAKAGAWA T, USAMI S, SHINKAWA H, OTTERSEN OP (1999) Immunoelectron microscopy of AMPA receptor subunits reveals three types of putative glutamatergic synapse in the rat vestibular end organs. Brain Res 819:58–64

MATSUGAMI TR, TANEMURA K, MIEDA M, NAKATOMI R, YAMADA K, KONDO T, OGAWA M, OBATA K, WATANABE M, HASHIKAWA T, TANAKA K (2006) From the Cover: Indispensability of the glutamate transporters GLAST and GLT1 to brain development. Proc Natl Acad Sci USA 103:12161–12166

OLIVER D, KNIPPER M, DERST C, FAKLER B (2003) Resting potential and submembrane calcium concentration of inner hair cells in the isolated mouse cochlea are set by KCNQ-type potassium channels. J Neurosci 23:2141–2149

PARK CK, CHA J, PARK SC, LEE PY, KIM JH, KIM HS, KIM SA, KIM IB, CHUN MH (2009) Differential expression of two glutamate transporters, GLAST and GLT-1, in an experimental rat model of glaucoma. Exp Brain Res 197:101–109

PEGHINI P, JANZEN J, STOFFEL W (1997) Glutamate transporter EAAC-1-deficient mice develop dicarboxylic aminoaciduria and behavioral abnormalities but no neurodegeneration. EMBO J 16:3822–3832

ROCHA-SANCHEZ SM, MORRIS KA, KACHAR B, NICHOLS D, FRITZSCH B, BEISEL KW (2007) Developmental expression of Kcnq4 in vestibular neurons and neurosensory epithelia. Brain Res 1139:117–125

ROTHSTEIN JD, MARTIN L, LEVEY AI, DYKES-HOBERG M, JIN L, WU D, NASH N, KUNCL RW (1994) Localization of neuronal and glial glutamate transporters. Neuron 13:713–725

ROTHSTEIN JD, DYKES-HOBERG M, PARDO CA, BRISTOL LA, JIN L, KUNCL RW, KANAI Y, HEDIGER MA, WANG Y, SCHIELKE JP, WELTY DF (1996) Knockout of glutamate transporters reveals a major role for astroglial transport in excitotoxicity and clearance of glutamate. Neuron 16:675–686

RUTTIGER L, SAUSBIER M, ZIMMERMANN U, WINTER H, BRAIG C, ENGEL J, KNIRSCH M, ARNTZ C, LANGER P, HIRT B, MULLER M, KOPSCHALL I, PFISTER M, MUNKNER S, ROHBOCK K, PFAFF I, RUSCH A, RUTH P,

KNIPPER M (2004) Deletion of the Ca2+-activated potassium (BK) alpha-subunit but not the BKbeta1-subunit leads to progressive hearing loss. Proc Natl Acad Sci USA 101:12922–12927

SAFIEDDINE S, WENTHOLD RJ (1999) SNARE complex at the ribbon synapses of cochlear hair cells: analysis of synaptic vesicle- and synaptic membrane-associated proteins. Eur J Neurosci 11:803–812

SARTHY VP, PIGNATARO L, PANNICKE T, WEICK M, REICHENBACH A, HARADA T, TANAKA K, MARC R (2005) Glutamate transport by retinal Muller cells in glutamate/aspartate transporter-knockout mice. Glia 49:184–196

SCHUG N, BRAIG C, ZIMMERMANN U, ENGEL J, WINTER H, RUTH P, BLIN N, PFISTER M, KALBACHER H, KNIPPER M (2006) Differential expression of otoferlin in brain, vestibular system, immature and mature cochlea of the rat. Eur J Neurosci 24:3372–3380

SHIMIZU Y, HAKUBA N, HYODO J, TANIGUCHI M, GYO K (2005) Kanamycin ototoxicity in glutamate transporter knockout mice. Neurosci Lett 380:243–246

SOUSA AD, ANDRADE LR, SALLES FT, PILLAI AM, BUTTERMORE ED, BHAT MA, KACHAR B (2009) The septate junction protein caspr is required for structural support and retention of KCNQ4 at calyceal synapses of vestibular hair cells. J Neurosci 29:3103–3108

STOFFEL W, KORNER R, WACHTMANN D, KELLER BU (2004) Functional analysis of glutamate transporters in excitatory synaptic transmission of GLAST1 and GLAST1/EAAC1 deficient mice. Brain Res Mol Brain Res 128:170–181

STORCK T, SCHULTE S, HOFMANN K, STOFFEL W (1992) Structure, expression, and functional analysis of a Na(+)-dependent glutamate/aspartate transporter from rat brain. Proc Natl Acad Sci USA 89:10955–10959

TAKAMORI S, RHEE JS, ROSENMUND C, JAHN R (2000) Identification of a vesicular glutamate transporter that defines a glutamatergic phenotype in neurons. Nature 407:189–194

TAKASAKI C, OKADA R, MITANI A, FUKAYA M, YAMASAKI M, FUJIHARA Y, SHIRAKAWA T, TANAKA K, WATANABE M (2008) Glutamate transporters regulate lesion-induced plasticity in the developing somatosensory cortex. J Neurosci 28:4995–5006

TAKUMI Y, MATSUBARA A, DANBOLT NC, LAAKE JH, STORM-MATHISEN J, USAMI S, SHINKAWA H, OTTERSEN OP (1997) Discrete cellular and subcellular localization of glutamine synthetase and the glutamate transporter GLAST in the rat vestibular end organ. Neuroscience 79:1137–1144

TSURU N, UEDA Y, DOI T (2002) Amygdaloid kindling in glutamate transporter (GLAST) knockout mice. Epilepsia 43:805–811

USAMI S, OTTERSEN OP (1995) Differential cellular distribution of glutamate and glutamine in the rat vestibular endorgans: an immunocytochemical study. Brain Res 676:285–292

USAMI S, OSEN KK, ZHANG N, OTTERSEN OP (1992) Distribution of glutamate-like and glutamine-like immunoreactivities in the rat organ of Corti: a light microscopic and semiquantitative electron microscopic analysis with a note on the localization of aspartate. Exp Brain Res 91:1–11

WAHLE S, STOFFEL W (1996) Membrane topology of the high-affinity L-glutamate transporter (GLAST-1) of the central nervous system. J Cell Biol 135:1867–1877

WATANABE T, MORIMOTO K, HIRAO T, SUWAKI H, WATASE K, TANAKA K (1999) Amygdala-kindled and pentylenetetrazole-induced seizures in glutamate transporter GLAST-deficient mice. Brain Res 845:92–96

WATASE K, HASHIMOTO K, KANO M, YAMADA K, WATANABE M, INOUE Y, OKUYAMA S, SAKAGAWA T, OGAWA S, KAWASHIMA N, HORI S, TAKIMOTO M, WADA K, TANAKA K (1998) Motor discoordination and increased susceptibility to cerebellar injury in GLAST mutant mice. Eur J Neurosci 10:976–988

WINTER H, BRAIG C, ZIMMERMANN U, GEISLER HS, FRANZER JT, WEBER T, LEY M, ENGEL J, KNIRSCH M, BAUER K, CHRIST S, WALSH EJ, MCGEE J, KOPSCHALL I, ROHBOCK K, KNIPPER M (2006) Thyroid hormone receptors TRalpha1 and TRbeta differentially regulate gene expression of Kcnq4 and prestin during final differentiation of outer hair cells. J Cell Sci 119:2975–2984

ZHANG FX, PANG YW, ZHANG MM, ZHANG T, DONG YL, LAI CH, SHUM DK, CHAN YS, LI JL, LI YQ (2010) Expression of vesicular glutamate transporters in peripheral vestibular structures and vestibular nuclear complex of rat. Neuroscience 173:179–189